Surface-Enhanced Decomposition Kinetics of Molecular Materials Illustrated with Cyclotetramethylene-tetranitramine

ARTICLE *in* THE JOURNAL OF PHYSICAL CHEMISTRY C · MAY 2012

Impact Factor: 4.77 · DOI: 10.1021/jp301723j

2 AUTHORS:

Onise Sharia
University of Notre Dame
35 PUBLICATIONS **372** CITATIONS
SEE PROFILE

Maija M. Kuklja
University of Maryland, College Park
115 PUBLICATIONS **1,671** CITATIONS
SEE PROFILE

THE JOURNAL OF PHYSICAL CHEMISTRY C

Article

pubs.acs.org/JPCC

Surface-Enhanced Decomposition Kinetics of Molecular Materials Illustrated with Cyclotetramethylene-tetranitramine

Onise Sharia and Maija M. Kuklja*

Department of Materials Science and Engineering, University of Maryland, College Park, Maryland 20742, United States

ABSTRACT: First principles total energy calculations were combined with variational transition state theory to reveal a surface-induced effect on the decomposition of a molecular material. Explored decomposition reactions were illustrated with energetic molecular solid β-cyclotetramethylene-tetranitramine. Simulated N−NO_2 homolysis reactions demonstrated that initiation of molecular material's degradation is characterized by a reduced activation barrier and significantly accelerated reaction rates for molecules that are placed on a free surface, an internal void, or a vacancy as compared to the perfect bulk crystal.

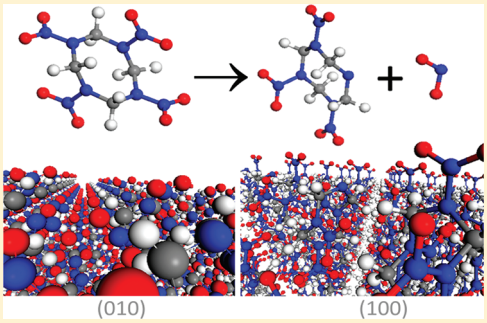

I. INTRODUCTION

Molecular materials exhibit a stunning diversity of functions, encapsulating magnetic, optical, and electrical properties. With applications in energy conversion and storage, microelectronics, optoelectronics and photonics, quantum information processing, nanotechnology and data storage, medicine and security, molecular materials enrich our every-day lives in many ways. While molecular materials present a large array of distinct complex arrangements in which small, delicate changes in a molecular structure can totally alter the properties of the material in bulk, they still have clear similarities. Molecules in highly ordered molecular crystals are held together by weak intermolecular interactions, whereas atoms in molecules are bound by strong chemical bonds. The chemistry of surfaces and interfaces is especially important in all molecular materials.

Among organic molecular crystals, a special place belongs to high energy density materials that store large amounts of chemical energy that can be rapidly transformed into thermal and mechanical energy upon external perturbation. Decomposition reactions proceed violently, releasing huge amounts of thermal energy. Although energetic materials have for quite some time now been used in devices for a wide range of applications, their enormous potential is not fully utilized. Despite many recent advances in the field,[1−3] the chemistry of processes underlying initiation of the energy release is not completely understood.[4,5] For example, the details of decomposition mechanisms in energetic solids and correlations between the structure, lattice stability, and potential ways and conditions that trigger the materials' degradation are yet to be established. A better understanding of such correlations would open up vastly new opportunities in modern science and technology.

In the meantime, even a "simple" question of the nature of the very initial step in the decomposition process of energetic materials remains subject of animated debate (see, for example, refs 6−10). Most researchers however agree that defects and deformations play a role.[6,11] Recent studies suggested that vacancies,[12,13] shear-strain interfaces,[14−17] dislocations,[18,19] charged particles,[20,21] and electronic excitations[21−26] are imperative in initiating chemical reactions in energetic materials by facilitating their degradation. First principles calculations of defects in energetic solids, which proved to be instrumental for elucidation of mechanisms of fast chemistry that are not attainable from experiment alone, became practical and available only during the past decade.[12,15−17,19−21,24−26] Among many factors affecting the sensitivity of materials to external perturbation triggering chemical reactions are a density and an exposed surface area. The surface chemistry is particularly difficult to tackle both experimentally and theoretically.

In this article, we further advance the previously developed strategy of calculating reaction rates for decomposition of isolated molecules[28] and ideal bulk crystals[27] by means of density functional theory (DFT) coupled with variational transition state theory. We now extend this technique to reveal a surface- and vacancy-induced effect on chemical decomposition reactions in molecular crystals. A comparison of the theoretically obtained activation barriers and reaction rates of the solid-state decomposition process[27] and the gas-phase predicted that ideal crystals are more stable and decompose slower than isolated molecules;[28] this appears in contradiction with experiment and a widely accepted view that solids decompose faster than gas-phase materials.[7,11] This research demonstrates that the initiation of a rapid decomposition of energetic molecular materials favors molecules placed on surface interfaces, voids, or molecular vacancies because of reduced activation barriers and fast kinetics. The selected material, β-cyclo-tetramethylene-tetranitramine (octahydro-

Received: February 21, 2012
Revised: May 3, 2012
Published: May 7, 2012

1,3,5,7-tetranitro-1,3,5,7-tetrazocine or β-HMX), has been intensively studied, and hence, it serves as an ideal model system to analyze how chemical decomposition of molecular materials depends on local molecular surroundings.

II. DETAILS OF CALCULATIONS

In calculations, we used a plane wave DFT[29,30] in the GGA approximation with PBE[31] functional and Projector Augmented Wave[32] pseudopotentials as implemented in the VASP code.[33] The kinetic energy cutoff was set to 600 eV. For the HMX unit cell of 6.7 × 11.4 × 8.9 Å, we used 2 × 2 × 2 Monkhorst-Pack[34] *k*-point mesh, which was accordingly reduced for larger cells. Atomic positions were relaxed using the conjugate gradient and quasi-Newton methods within a force tolerance of 0.025 Å/eV. Minimal energy paths were calculated using the climbing nudged elastic band method[35] with six intermediate images. The computationally obtained structure of β-HMX was found to be in agreement with the experimental data within 1−3%.[27]

To explore the surface chemistry, we represent the HMX crystal using a slab model in which the supercell was composed of four molecular HMX layers and 10 Å of vacuum in the *z* direction (Figure 1). The large 16 molecule supercells used in the calculations ensure that spurious interactions between adjacent cells are negligible and do not affect the modeling of chemical reactions.

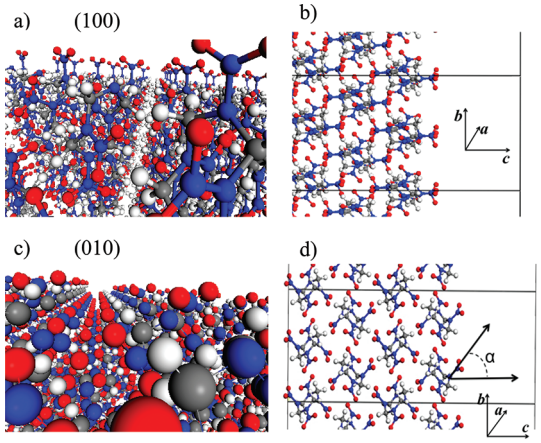

Figure 1. HMX surface slab models are shown: (a) (100) surface, (b) (100) slab super cell model, with the parameters of the slabcut of $a = b = 14.47$ Å, $c = 34.43$ Å, $\alpha = \beta = 90°$, and $\gamma = 104.03°$; (c) (010) surface, and (d) (010) slab super cell model, with the parameters of the slabcut of $a = 15.164$, $b = 13.4654$, $c = 32.6824$, $\alpha = \beta = 90°$, and $\gamma = 76.704$. The angle α between the N−NO_2 bond and the normal of the (100) surface is 77° and of the (010) surface is 38°.

III. KINETICS OF THE N−NO_2 HOMOLYSIS

It was established that N−NO_2 homolysis is a dominating decomposition reaction in both the gas-phase[28] and perfect crystals;[27,36] hence, we will focus here only on this mechanism for surface chemistry and ignore for now all other possible decomposition channels. The molecular structure of β-HMX consists of an eight-membered ring of alternating carbon and nitrogen atoms, with two equatorial and two axial nitro groups attached to nitrogen atoms (Figure 2). To simulate their splitting off of the molecule and probe whether they behave differently, we considered two relevant surfaces in HMX (Figure 1a−d). The (100) surface cuts the crystal along the

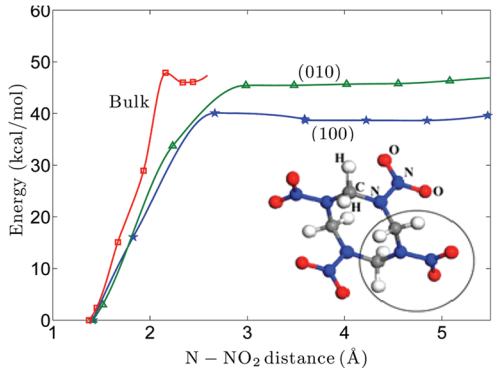

Figure 2. Minimum energy paths for N−NO_2 homolysis and the atomic structure of HMX molecule.

direction of the *axial* N−NO_2 bond, and the (010) surface is covered by *equatorial* NO_2 groups as illustrated in Figure 1a−d. The full atomic relaxation leads to the axial N−NO_2 bond to elongate from 1.373 Å in bulk to 1.411 Å at the surface and the equatorial N−NO_2 bond to change from 1.391 to 1.413 Å. The different outward relaxations of NO_2 groups at the (100) and (010) surfaces are also reflected in different surface energies γ calculated as: $\gamma = 1/2A(E_{total} - n_{HMX}E_{HMX})$, where E_{total} is the total energy, A is the surface area, n_{HMX} is the number of HMX molecules in the system, and E_{HMX} is the normalized energy of the bulk HMX per molecule. The obtained energies of the (100) and (010) surfaces are 69.05 and 44.09 mJ/m^2, respectively; the last is in agreement with the experimental (010) surface energy of 46 mJ/m^2 [37,38].

The N−NO_2 homolysis was modeled by extending the N−NO_2 bond to 5.5 Å for the (100) surface and 5.1 Å for the (010) surface. To eliminate a possible recombination of the NO_2 group with its parent HMX molecule, we fix the N atom of the nitro-group and let the rest of atoms relax. At the indicated distance, the N−NO_2 bond was dissociated, and the system relaxed to a triplet state for both surface orientations, similarly to its behavior in the gas and crystalline phases.[27,28] The N−NO_2 homolysis at the (100) surface requires 40.2 kcal/mol and exhibits a negligible barrier of 1.16 kcal/mol (Figure 2). The reaction energy for the decomposition of an equatorial nitro-group at the (010) surface is 46.3 kcal/mol and proceeds with no barrier. The calculated N−NO_2 homolysis activation energy on either surface is comparable with that in the gas phase (42.8 and 44.6 kcal/mol)[28] and is lower than the activation barrier in a perfect solid bulk HMX (47.9 kcal/mol)[27] (Table 1). On the basis of energetic considerations, the surface decomposition favors the axial nitro group over the equatorial group. In addition, the observed difference in energy

Table 1. Activation Barriers and Reaction Rate Constants for N−NO_2 Homolysis of an HMX Molecule Placed in the Gas Phase, Bulk Crystal, at a Surface, and at a Vacancy[a]

	barrier (kcal/mol)		rate constant log (k/s^{-1})	
N−NO_2 homolysis	axial	equatorial	axial	equatorial
gas phase	42.8 (38.1)	44.6 (40.1)	17.8	18.7
bulk crystal	47.9 (43.7)	>65	15.1	
surface	40.1 (37.4)	46.3 (42.2)	17.3	18.2
vacancy	41.0 (36.5)	44.2 (39.5)	18.9	18.8

[a]Zero-point corrected energy is given in parentheses.

dx.doi.org/10.1021/jp301723j | J. Phys. Chem. C 2012, 116, 11077−11081

is consistent with HMX surface variability and offers a simple explanation to large variations in experimental activation barrier data[7] (vide infra).

Further, we simulated a single molecular vacancy by removing one HMX molecule from a 2 × 2 × 2 16 molecule supercell. This corresponds to 6.25% concentration of vacancies in the material. After the lattice relaxation due to the vacancy, a small elongation of the N−NO_2 bond length was observed. The calculated activation energy required for the axial and equatorial nitro-group homolysis is 40.0 and 44.2 kcal/mol, respectively.

Now, we explore the reaction kinetics. Rates of reactions with a well-defined transition state and the barrier height E_B, can be described by conventional transition state theory:[39]

$$k = \frac{k_B T}{h}\frac{Z^{TS}}{Z^0} e^{-E_B/k_B T} \quad (1)$$

where Z^{TS} and Z^0 are partition functions for the system at the transition point and in the initial configuration, respectively, k_B is Boltzmann constant, h is Planck's constant, and T is the temperature. For reactions that do not have a transition state, such as the N−NO_2 homolysis, the k may be obtained by means of variational transition state theory.[40] In this case, a set of potential pseudotransition states is defined first and the one yielding a minimal value of k is chosen. In general, it is difficult to calculate Z^{TS}. To overcome this difficulty for the N−NO_2 homolysis, we assume that (1) the NO_2 can decompose in any forward direction with equal probability and (2) after the NO_2 splits from the HMX, the nitro-group can rotate freely. To validate those assumptions, we conducted some test calculations. We modeled and analyzed minimal energy pathways of the N−NO_2 decomposition on the (100) surface in two arbitrarily chosen directions, along the N−NO_2 bond and at 60° with respect to the first path. Both obtained pathways exhibited a remarkable similarity in behavior. Hence, the N−NO_2 fission in any forward direction is equally probable to a good approximation. A comparison of the total energies of the system for various orientations of the NO_2 revealed that the energy change did not exceed 0.5 kcal/mol. This demonstration allows us to consider the NO_2 molecule as a free rotor. Using the aforementioned assumptions, we derive

$$k = \frac{Z_{rot}^{NO_2} Z_{vib}^{TS}}{Z_{vib}^{0}} \frac{6 m_{NO_2} \pi r^2 (k_B T)^2}{h^3} e^{-E_B/k_B T} \quad (2)$$

here Z^{NO_2} is a partition function of the NO_2 in a free rotor approximation, m_{NO_2} is mass of the NO_2 molecule, and r is the distance for which the rate becomes minimal (it varies from 2.5 to 3.5 Å depending on temperature, we choose r equal to 3 Å).

Calculations of partition functions in a harmonic approximation require the determination of vibrational frequencies at the initial and transition points. Because of the large size of our system, this is a computationally extremely challenging task. We circumvent this problem by limiting the number of vibrations and considering vibrations of only those atoms that directly participate in the dissociation reactions. In this case, we allow only ten atoms to vibrate, as shown in Figure 2 and froze all other atoms. Our estimate shows that the numerical error of the pre-exponential factor induced by this approximation does not exceed 0.3 (2%).

Table 1 summarizes the results of our calculations. Similarly to the gas phase decomposition, there is obvious discrimination between nitro groups with the axial group favored over the equatorial group. An important conclusion obtained here is that the decomposition of the surface molecules requires a significantly smaller energy than molecules buried in the crystal and even slightly smaller than gas-phase molecules. Most importantly, the N−NO_2 homolysis reactions of the HMX molecule placed at a surface or at a vacancy develop 2−4 orders of magnitude faster than those in a perfect solid and are comparable to or somewhat faster than the gas phase reactions. The appreciable difference in the dissociation activation energies of the axial nitro group versus the equatorial nitro group suggests that significant variations in activation barriers registered in experiments[7,41] can be in part explained by many possible surfaces of HMX crystals observed,[14,18,37] together with a small heat of evaporation (28 kcal/mol).[42]

A single vacancy has a similar effect on the N−NO_2 homolysis reaction as the surface. This finding is consistent with insight originally suggested in the earlier work[12] performed on cyclotrimethylene-trinitramine (RDX), relevant to HMX material, and indeed confirms that the reaction kinetics of a dissociating molecule is strongly dependent upon the molecular environment. The imbalance of intermolecular interactions induced by a free surface, an internal void, and even a simple molecular vacancy causes a barrier reduction and accelerated reaction rates as the decomposing molecule is only partly bonded to its neighbors. This implies that the decomposition of HMX and other energetic materials is likely to start at surfaces, interfaces, and voids.

We note that caution must be exercised when comparing our calculated kinetics with experiment due to (i) the ideal, defect-free arrangement of the materials having only vacancies or voids modeled here can hardly be expected from real samples and (ii) thermal decomposition experiments measure only aggregate materials degradation and do not distinguish between individual reactions. With this caveat, our results should be considered in agreement with experiment. All calculated solid state reaction barriers for HMX thermal decomposition are within the experimentally reported range from 13 to 67 kcal/mol.[41] The calculated reaction constants also fall into the measured range from 2.5 to 25 s^{-1} [41]. The most recent experiments registered the narrower range of activation barriers from 23 to 46.6 kcal/mol, with the most reliable data obtained from 33.7 to 46.6 kcal/mol and reaction constants from 8.5 to 17.0 s^{-1} [43]. Our calculations are also consistent with recent ReaxFF molecular dynamic simulations,[44] which suggested that molecular vacancies accelerate the decomposition of condensed-phase HMX.

Interestingly enough, our ab initio modeling of surface kinetics reconciles the seeming contradiction between simulations of condensed HMX[27] and experiment[7] and predicts that porous HMX should be more sensitive to the thermal treatment and decompose faster than solid samples. The obtained results also suggest a simple and consistent interpretation to a dispersion of the available experimental results of activation barriers and reaction kinetics. Surface roughness, open pores, cracks and other imperfections that increase the surface area would also make the material more sensitive. This can be quantified precisely by expressing the obtained here reaction kinetics via a fraction of molecules placed on open surfaces or voids in practical samples.

IV. CONCLUSIONS

The surface- and vacancy-enhanced kinetics of the chemical decomposition of molecular materials is revealed by means of first principles electronic structure calculations combined with

dx.doi.org/10.1021/jp301723j | J. Phys. Chem. C 2012, 116, 11077−11081

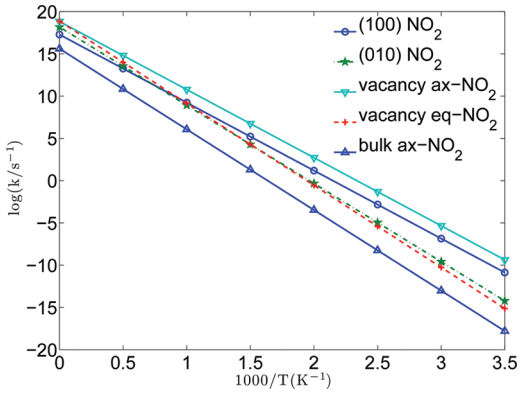

Figure 3. Calculated reaction rates are compared for N−NO_2 homolysis taking place on surfaces, vacancies, and in bulk HMX crystal.

variational transition state theory. The major conclusion that the thermal decomposition favors molecules placed on surfaces and interfaces because of reduced activation barriers and fast kinetics is explained by the delicate interplay of inter- and intramolecular interactions in a molecular crystal. The technique of calculating kinetic parameters of the solid-state decomposition process is illustrated with the energetic material HMX; however, the approach can be easily generalized to other molecular, supramolecular, and hierarchical materials and complex systems. The results of this work serve as the foundation for understanding such complex issues of surface chemistry as materials (in)stability, thermal explosion experiments, rapid degradation under extreme and harsh conditions, and ultrafast chemical reactions.

AUTHOR INFORMATION

Corresponding Author

*Fax: (301)-314-2029. Tel: (301)-405-4646. E-mail: mkukla@umd.edu, mkukla@nsf.gov.

Notes

The authors declare no competing financial interest.

ACKNOWLEDGMENTS

This research is supported in part by ONR (Grant N00014-12-1-0529) and NSF. We used NSF XSEDE resources (Grant DMR-100054) and DOE NERSC resources (Contract DE-AC02-05CH11231). M.M.K. is grateful to the Office of the Director of NSF for support under the IRD program. Any appearance of findings, conclusions, or recommendations, expressed in this material are those of the authors and do not necessarily reflect the views of NSF.

REFERENCES

(1) Dlott, D. D. *Annu. Rev. Phys. Chem.* **2011**, *62*, 575−597.
(2) Bhattacharya, A.; Guo, Y.; Bernstein, E. R. *Acc. Chem. Res.* **2010**, *43*, 1476−1485.
(3) Steinhauser, G.; Klapotke, T. M. *Angew. Chem., Int. Ed.* **2008**, *47*, 3330−3347.
(4) Oran, E. S.; Williams, F. A. *Philos. Trans. R. Soc., A* **2012**, *370*, 534−543.
(5) An, Q.; Zybin, S. V.; Goddard, W. A.; Jaramillo-Botero, A.; Blanco, M.; Luo, S. N. *Phys. Rev. B* **2011**, *84*, 220101−220105.
(6) Bowden, F. P. Yoffe, A. D. *Fast Reactions in Solids*; Butterworth Press: London, 1958.
(7) Brill, T. B.; James, K. J. *Chem. Rev.* **1993**, *93*, 2667−2692.
(8) Piekiel, N.; Zachariah, M. R. *J. Phys. Chem. A* **2012**, *116*, 1519−1526.
(9) Zhu, W. H.; Huang, H.; Huang, H. J.; Xiao, H. M. *J. Chem. Phys.* **2012**, *136*, 044516−6.
(10) Korolev, V. L.; Pivina, T. S.; Porollo, A. A.; Petukhova, T. V.; Sheremetev, A. B.; Ivshin, V. P. *Russ. Chem. Rev.* **2009**, *78*, 945−969.
(11) Walley, S. M.; Field, J. E.; Greenaway, M. W. *Mater. Sci. Technol.* **2006**, *22*, 402−413.
(12) Kuklja, M. M. *J. Phys. Chem. B* **2001**, *105*, 10159−10162.
(13) Boyd, S.; Murray, J. S.; Politzer, P. *J. Chem. Phys.* **2009**, *131*, 204903−7.
(14) Armstrong, R. W.; Elban, W. L. *Mater. Sci. Technol.* **2006**, *22*, 381−395.
(15) Kuklja, M. M.; Rashkeev, S. N. *J. Phys. Chem. C (lett)* **2009**, *113*, 17−20.
(16) Kuklja, M. M.; Rashkeev, S. N. *J. Phys. Chem. Lett.* **2010**, *1*, 363−367.
(17) Kuklja, M. M.; Rashkeev, S. N.; Zerilli, F. J. *Appl. Phys. Lett.* **2006**, *89*, 071904−3. Kuklja, M. M.; Rashkeev, S. N. *Appl. Phys. Lett.* **2007**, *90*, 151913−3.
(18) Armstrong, R. W. *Rev. Adv. Mater. Sci.* **2009**, *19*, 13−40.
(19) Kuklja, M. M.; Kunz, A. B. *J. Appl. Phys.* **2001**, *89*, 4962−4970; **2000**, *87*, 2215−2218.
(20) Kunz, A. B.; Beck, D. R. *Phys. Rev. B.* **1987**, *36*, 7580−7585.
(21) Kimmel, A. V.; Sushko, P. V.; Shluger, A. L.; Kuklja, M. M. *J. Chem. Phys.* **2007**, *126*, 234711−234711-10.
(22) Reed, E. J. *J. Phys. Chem. C* **2012**, *116*, 2205−2211.
(23) Bhattacharya, A.; Guo, Y. Q.; Bernstein, E. R. *J. Phys. Chem. A* **2009**, *113*, 811−823. Bhattacharya, A.; Bernstein, E. R. *J. Phys. Chem. A* **2011**, *115*, 4135−4147.
(24) Kuklja, M. M.; Stefanovich, E. V.; Kunz, A. B. *J. Chem. Phys.* **2000**, *112*, 3417−3423.
(25) Kuklja, M. M. *Appl. Phys. A: Mater. Sci. Process.* **2003**, *76* (3), 359−366.
(26) Aluker, E. D.; Krechetov, A. G.; Mitrofanov, A. Y.; Nurmukhametov, D. R.; Kuklja, M. M. *J. Phys. Chem. C* **2011**, *115* (14), 6893−6901.
(27) Sharia, O.; Kuklja, M. M. *J. Phys. Chem. B* **2011**, *115*, 12677−12686.
(28) Sharia, O.; Kuklja, M. M. *J. Phys. Chem. A* **2010**, *114*, 12656−12661.
(29) Hohenberg, P.; Kohn, W. *Phys. Rev.* **1964**, *136*, B864−B871.
(30) Kohn, W.; Sham, L. J. *Phys. Rev. A* **1965**, *140*, A1133−A1138.
(31) Perdew, J. P.; Burke, K.; Ernzerhof, M. *Phys. Rev. Lett.* **1996**, *77*, 3865−3868.
(32) Blöchl, P. E. *Phys. Rev. B* **1994**, *50*, 17953−17979.
(33) Kresse, G; Furthmuller, J *Comput. Mater. Sci.* **1996**, *6*, 15−50. Kresse, G; Furthmuller, F *Phys. Rev. B* **1996**, *54*, 11169−11186. Kresse, G.; Hafner, J. *Phys. Rev. B* **1993**, *47*, RC558.
(34) Monkhorst, H. J.; Pack, J. D. *Phys. Rev. B* **1976**, *13*, 5188−5192.
(35) Henkelman, G.; Uberuaga, B. P.; Jónsson, H. *J. Chem. Phys.* **2000**, *113*, 9901−9904.
(36) Zhang, L. Z.; Zybin, S. V.; van Duin, A. C. T.; Dasgupta, S.; Goddard, W. A., III *J. Phys. Chem. A* **2009**, *113*, 10619−10640.
(37) Elban, W. L. *J. Mater. Sci.* **1979**, *14* (4), 1008−1011.
(38) Yee, R. Y.; Adicoff, A.; Dibble, E. J. Surface properties of HMX crystal. Presented at the 17th Combustion Meetings: Papers JANNAF, 1980.
(39) Hanggi, P.; Talkner, P.; Borkovec, M. *Rev. Mod. Phys* **1990**, *62*, 251−341.
(40) Garrett, B. C.; Truhlar, D. G. *J. Phys. Chem.* **1979**, *83*, 1079−1112.
(41) Brill, T. B.; Arisawa, H.; Brush, P. J.; Gongwer, P. E.; Williams, G. K. *J. Phys. Chem.* **1995**, *99*, 1384−1392.
(42) Sinditskii, V. P.; Egorshev, V.Yu.; Serushkin, V. V.; Levshenkov, A. I.; Berezin, M. V.; Filatov, S. A.; Smirnov, S. P. *Thermochim. Acta* **2009**, *496*, 1−12.
(43) Glascoe, E. A.; Hsu, P. C.; Springer, H. K.; DeHaven, M. R.; Tan, N.; Turner, H. C. *Thermochim. Acta* **2011**, *515*, 58−66.

(44) Zhou, T.-T.; Huang, F.-L. *J. Phys. Chem. B* **2011**, *115*, 278−287.